

THE EFFECT OF COMMON DESIGN PARAMETERS ON THE
THERMAL PERFORMANCE OF MICROELECTRONIC EQUIPMENT:
PART I – NATURAL CONVECTION

S. Lee, J. R. Culham, and M. M. Yovanovich
Department of Mechanical Engineering
Microelectronics Heat Transfer Laboratory
University of Waterloo
Waterloo, Ontario, Canada

ABSTRACT

Many microelectronic applications employ natural convection cooling as the sole means of dissipating heat due to the simplicity of the process and the low long term costs associated with maintenance and reliability. But the trend in microelectronic design towards higher packaging densities and higher power dissipation rates often leads to circuit board temperatures which exceed predetermined limitations, which have been established to ensure long term reliability. In order to maintain operating temperatures at safe levels, designers must be aware of the significance that each design decision has on the rate of heat transfer and in turn the final operating temperature of circuit board components. The purpose of this paper is to determine the parameters on which the operating temperature depends and to show the effect that these parameters, such as the thermophysical properties, package location, and the applied power level, have on localized temperature and the average Nusselt number.

NOMENCLATURE

- Bi Biot number $\equiv ht/k$,
- Bq Boussinesq number $\equiv g\beta L^4 q/k_f \alpha^2$
- c_p specific heat, J/kgK
- d dimensionless distance between heat sources
- g gravitational acceleration, m/s²
- h convective heat transfer coefficient, W/m²K
- k thermal conductivity, W/mK
- ℓ heat source length and width, m
- L total circuit board length, m
- Nu Nusselt Number $\equiv q\ell/(T - T_\infty)k_f$
- Pr Prandtl number $\equiv \nu/\alpha$
- q heat flux, W/m²
- Q heat transfer rate, W
- t circuit board thickness, m
- T temperature, K

- u, v, w flow velocity in the x, y, z -direction, m/s
- W total circuit board width, m
- x, y, z Cartesian coordinates

Greek Symbols

- α thermal diffusivity $\equiv k_f/\rho c_p$, m²/s
- β thermal expansion coefficient, K⁻¹
- ϵ emissivity
- ρ density, kg/m³
- θ dimensionless temperature excess
- ν kinematic viscosity, m²/s
- σ Stefan-Boltzmann constant $\equiv 5.67 \times 10^{-8}$, W/m² K⁴
- ϕ dimensionless temperature change, see Eq. (33)

Subscripts

- c circuit board center line
- f fluid
- j Joulean heat generation
- r radiation
- s solid
- sur surrounding condition
- w wall condition
- 1 upstream heat source
- 2 downstream heat source
- ∞ free stream condition

Superscripts

- * dimensionless variable

INTRODUCTION

The prediction of operating temperatures and heat transfer performance in microelectronic circuit boards, necessitates the use of a conjugate heat transfer model which accounts for

the simultaneous occurrence of convection into the cooling fluid, conduction through the circuit board, and radiation heat transfer to the surroundings. Conjugate problems involving natural convection heat transfer from a vertical plate immersed in an extensive fluid have not received much attention to date. Most existing studies in the literature deal with two-dimensional analyses, by ignoring or excluding the effect of the third dimension in the direction across the width of the plate. Zinnes (1970) solved two-dimensional conjugate problems with strip heat sources using finite difference methods and compared the surface temperature variations with experimental results. Further studies were carried out by Kishinami and Seki (1983), and Kishinami et al. (1987) using both numerical and experimental methods. Lee and Yovanovich (1989) obtained analytical solutions for two-dimensional conjugate problems using an approximate method and reported excellent agreement of the results with the numerical and experimental data of Zinnes (1970).

Although the detailed output data available from most state-of-the-art Computer Aided Design tools is of importance in establishing localized hot spots on the surface of a circuit board, the preliminary stages of circuit board design often requires more of a "feel" for the significance due to changes in various design parameters and not as much detail. The "feel" can be based on trends established from prior experimental testing, the estimation of upper and lower bound solutions based on analytical simplifications or, as is the intent of this paper, the presentation of a case study where a specific example is examined in detail to ascertain a better understanding of the relationship between basic design parameters and conjugate heat transfer in a circuit board.

THERMAL MODEL

A typical microelectronic circuit board, as shown in Fig. 1, consists of a multilayered substrate, formed from alternating layers of a conductive material, such as copper with layers of an insulating material, such as fiberglass/epoxy. Attached to the surface of the substrate are IC packages, resistors, capacitors and other heat generating devices. For the purpose of this

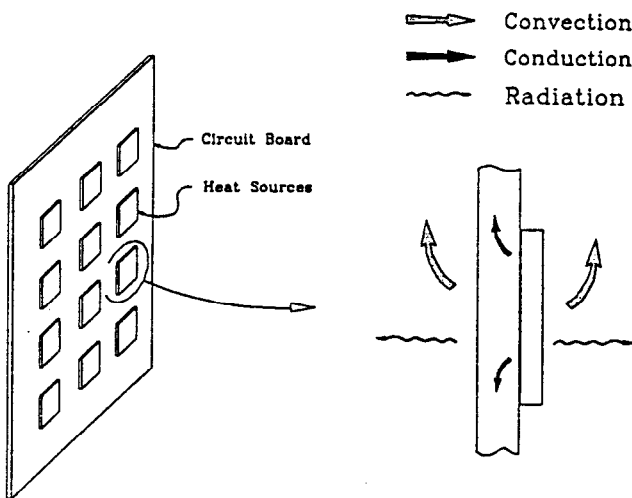


Fig. 1 Printed circuit board shown with schematic of thermal dissipation from heat sources.

study, the heat sources are assumed to be low profile, square packages in perfect contact with the substrate. The Joulean heating within each source is assumed to be uniform. Due to the complex temperature field established between the substrate, the heat sources and the surrounding air medium an exact analytical solution is not available with present solution techniques. However, approximate methods combined with a few simplifying assumptions will significantly reduce the difficulties associated with the solution technique and can be used to obtain accurate solutions to highly complex conjugate heat transfer problems.

Figure 2 shows a geometric configuration of the circuit board with two iso-flux heat sources and the coordinate system used in the following analysis. The circuit board is suspended in a quiescent fluid which is contained within surroundings of large extent. The fluid is assumed to be maintained at a uniform temperature T_∞ , and the surroundings, not shown in the figure, are also assumed to be at a uniform temperature, T_{sur} . For the present modeling, flush mounted heat sources are assumed, representative of chip-on-board or surface mount technology. Surface mount and chip-on-board technology eliminates the need to install component pins in pre-formed through-holes which must be filled with solder to provide electrical and mechanical integrity. Surface mount and chip-on-board technologies also permit components to be mounted closer to the surface of the circuit board, giving the overall surface of the circuit board a smooth appearance.

Fluid-Side Equations

The standard boundary layer equations, in which the transport of momentum and energy by diffusion processes is assumed negligible compared to convection in the direction parallel to the flow stream, will be used to describe the flow and energy field within the surrounding fluid. In addition to the implicit boundary layer approximations the following assumptions will be included in the present study.

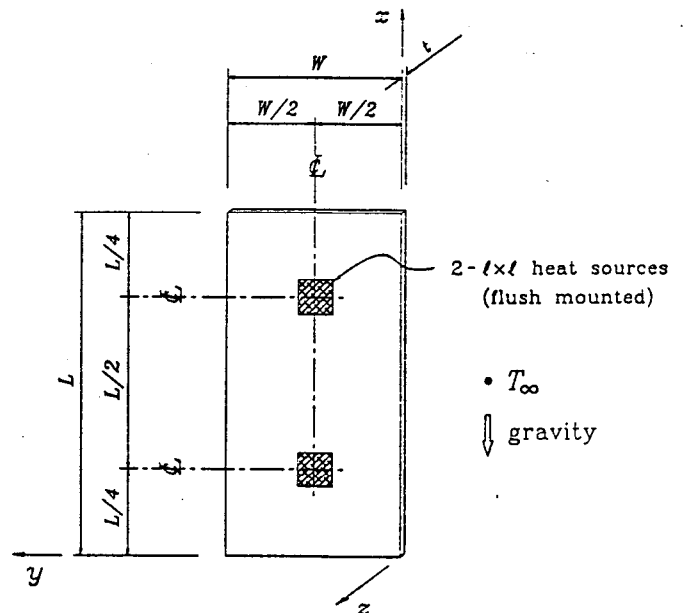


Fig. 2 Configuration and coordinate system of printed circuit board used as default case.

The v -velocity in the y -direction, across the width of the circuit board, is small compared to the buoyancy induced u -velocity in the x -direction. This combined with a scale analysis indicate that the convective transport in the y -direction can be ignored.

Thermophysical properties of the fluid, except the density variation used in the Boussinesq approximation, are assumed constant. The work done by the viscous force and the pressure work term are neglected. When air is used as a coolant fluid, its thermal conductivity is usually orders of magnitude smaller than that of the circuit board. As such, one can assume that the planar thermal diffusion parallel to the board surface (i.e., the x and y directions) is predominantly characterized by the conduction heat transfer in the circuit board. This not only supplements the validity of the boundary layer approximations but also allows one to ignore the planar diffusion of energy in the fluid, which in turn allows the planar diffusion of momentum to be ignored. Since the circuit board is thin and heat sources are usually mounted away from the edges of the circuit board, it is reasonable to assume that the operating temperature and the heat transfer characteristics of heating elements are not influenced by the edge effects. Based on the foregoing assumptions and approximations, the resulting governing equations become identical to the two-dimensional boundary layer equations in the x - z coordinates.

$$\frac{\partial u}{\partial x} + \frac{\partial w}{\partial z} = 0 \quad (1)$$

$$u \frac{\partial u}{\partial x} + w \frac{\partial u}{\partial z} = \nu \frac{\partial^2 u}{\partial z^2} + g\beta(T - T_\infty) \quad (2)$$

$$u \frac{\partial T}{\partial x} + w \frac{\partial T}{\partial z} = \alpha \frac{\partial^2 T}{\partial z^2} \quad (3)$$

where the following boundary conditions apply.

$$\text{as } z \rightarrow \pm\infty, \quad u \rightarrow 0, \quad T \rightarrow T_\infty \quad (4)$$

$$\text{at } x = 0, \quad u = 0, \quad T = T_\infty \quad (5)$$

$$\text{at } z = -t \text{ and } 0, \quad u = w = 0 \quad (6)$$

Although the assumption of negligible diffusion transport in the y -direction is invalid near the side-edges of the circuit board, and, for the same reason, the boundary layer approximations fail near the leading edge of the circuit board, the above equations can be considered applicable at any fixed y -location over the entire circuit board, for all practical purposes of the present investigation.

Solid-Side Equations

The governing equation for heat flow in a homogeneous solid body is Laplace's equation, given as

$$\frac{\partial^2 T}{\partial x^2} + \frac{\partial^2 T}{\partial y^2} + \frac{\partial^2 T}{\partial z^2} = 0 \quad (7)$$

where the boundary conditions, assuming negligible heat dissipation through the edge surfaces, are

$$\text{at } x = 0 \text{ and } L, \quad \frac{\partial T}{\partial x} = 0 \quad (8)$$

$$\text{at } y = 0 \text{ and } W, \quad \frac{\partial T}{\partial y} = 0 \quad (9)$$

And the interfacial conditions that couple the fluid/solid-side equations are

$$\text{at } z = -t \quad T_{(-t^+)} = T_{(-t^-)} \quad (10)$$

$$k_s \left. \frac{\partial T}{\partial z} \right|_{-t^+} = q_{r(-t)} + k_f \left. \frac{\partial T}{\partial z} \right|_{-t^-} \quad (11)$$

$$\text{at } z = 0 \quad T_{(0^-)} = T_{(0^+)} \quad (12)$$

$$k_s \left. \frac{\partial T}{\partial z} \right|_{0^-} = q_j - q_{r(0)} + k_f \left. \frac{\partial T}{\partial z} \right|_{0^+} \quad (13)$$

where q_r represents the radiative heat flux distribution over the front and back surface of the circuit board which can be expressed in terms of the Stefan-Boltzmann law of radiation,

$$q_r = \varepsilon\sigma(T_w^4 - T_{\text{sur}}^4) \quad (14)$$

where T_w denotes the local surface temperature of the circuit board at either $z = -t$ or $z = 0$. The subscripts $-t^+$ and 0^- denote the solid-side surfaces, and $-t^-$ and 0^+ denote the fluid-side surfaces at the fluid-solid interfaces.

The Joulean heat flux distribution, q_j , is an input function of x and y prescribed over the surface of the circuit board. It is obtained by dividing the total power input per heating element by the element surface area over the source locations and by assigning 0 over the non-heating regions.

If the Biot number based on the circuit board thickness ($Bi = ht/k_s$) is less than 0.1 the temperature gradient across the thickness of the board can be ignored without significantly altering the final solutions. In such cases, the interfacial conditions can be absorbed into the governing equations by integrating Laplace's equation across the thickness of the circuit board, and Eqs. (7), (11) and (13) reduce to a two-dimensional fin equation written as

$$\frac{\partial^2 T}{\partial x^2} + \frac{\partial^2 T}{\partial y^2} + \frac{1}{k_s t} \left(q_j - q_r + 2k_f \left. \frac{\partial T}{\partial z} \right|_{0^+} \right) = 0 \quad (15)$$

where $q_r = q_{r(-t)} + q_{r(0)}$.

META, a conjugate heat transfer modeling routine developed by Culham et al. (1991b) combines an approximate analytical boundary layer solution with a finite volume solid body solution, which takes advantage of the negligible temperature gradient across the thickness of a circuit board (i.e., $Bi < 0.1$), thereby allowing a two-dimensional solution to be used to solve for board temperatures. The boundary layer solution is based on a linearized form of the boundary layer equations (Lee and Yovanovich, 1991) for laminar flow over a flat plate with a flux specified boundary condition. The resulting formulation for the local heat transfer coefficient is then used as the surface convective condition in the solid body model, as presented by Lee and Yovanovich (1989). The two solutions are coupled using an

iterative procedure to give a unique temperature profile at the fluid-solid interface which simultaneously satisfies the governing equations described in the previous section for both the fluid and solid domains.

PARAMETRIC ANALYSIS

The above equations are non-dimensionalized by using the dimensionless parameters defined as

$$x^* = \frac{x}{L} \quad (16)$$

$$z^* = \frac{z}{L} \quad (17)$$

$$t^* = \frac{t}{L} \quad (18)$$

$$u^* = \frac{uL}{\nu} \quad (19)$$

$$w^* = \frac{wL}{\nu} \quad (20)$$

$$\theta = \frac{T - T_\infty}{\alpha^2/g\beta L^3} \quad (21)$$

Non-dimensionalizing the fluid-side equations

$$\frac{\partial u^*}{\partial x^*} + \frac{\partial w^*}{\partial z^*} = 0 \quad (22)$$

$$u^* \frac{\partial u^*}{\partial x^*} + w^* \frac{\partial u^*}{\partial z^*} = \frac{\partial^2 u^*}{\partial z^{*2}} + \frac{\theta}{Pr^2} \quad (23)$$

$$u^* \frac{\partial \theta}{\partial x^*} + w^* \frac{\partial \theta}{\partial z^*} = \frac{1}{Pr} \frac{\partial^2 \theta}{\partial z^{*2}} \quad (24)$$

with the boundary conditions

$$\text{as } z^* \rightarrow \pm\infty, \quad u^* \rightarrow 0, \quad \theta \rightarrow 0 \quad (25)$$

$$\text{at } x^* = 0, \quad u^* = 0, \quad \theta = 0 \quad (26)$$

$$\text{at } z^* = -t^* \text{ and } 0, \quad u^* = w^* = 0 \quad (27)$$

The corresponding two-dimensional solid-side equation becomes

$$\frac{k_s t}{k_f L} \left[\frac{\partial^2 \theta}{\partial x^{*2}} + \frac{\partial^2 \theta}{\partial y^{*2}} \right] + Bq_j - Bq_r + 2 \frac{\partial \theta}{\partial z^*} \Big|_{0^+} = 0 \quad (28)$$

with

$$\text{at } x^* = 0 \text{ and } 1, \quad \frac{\partial \theta}{\partial x^*} = 0 \quad (29)$$

$$\text{at } y^* = 0 \text{ and } \frac{W}{L}, \quad \frac{\partial \theta}{\partial y^*} = 0 \quad (30)$$

where Bq is the Boussinesq number defined as

$$Bq = \frac{g\beta L^4 q}{k_f \alpha^2} \quad (31)$$

with Bq_j based on q_j, and Bq_r based on q_r.

From the above equations the functional dependency of the dimensionless surface temperature can be written as

$$\theta_w = \theta_w(x^*, y^*, \frac{W}{L}, Pr, \frac{k_s t}{k_f L}, Bq_r, Bq_j) \quad (32)$$

This is an implicit non-linear equation due to the radiation heat transfer denoted by Bq_r which contains a fourth-order term of θ_w . Although the above function depends only on five dimensionless parameters, excluding the local positional parameters, the major difficulty in presenting and summarizing the parametric behavior of the surface temperature rests on the fact that one of the input parameters, namely Bq_j, itself is a function of x^* and y^* .

When Bi is greater than 0.1, the three-dimensional solid equation must be solved and the surface temperature depends on an additional parameter as the parameter $k_s t/k_f L$ decomposes to k_s/k_f and t/L .

DEFAULT CONDITIONS

Because of the inherent complexity of microelectronic circuit boards and the arrangement of IC packages, an endless combination of configurations could be selected for this study. Instead, a conventional two heat source circuit board, as shown in Fig. 2, will be analyzed, where dimensions and thermophysical properties for the default case are given as

$$\text{Board} : L \times W \times t = 0.2 \text{ m} \times 0.1 \text{ m} \times 0.0016 \text{ m}$$

$$k_s = 2 \text{ W/mK}$$

$$\epsilon = 0$$

$$\text{Heat Sources} : \ell \times \ell = 0.02 \text{ m} \times 0.02 \text{ m}$$

$$\epsilon = 0$$

$$Q_{j1} = Q_{j2} = 1 \text{ W}$$

$$\text{Fluid} : k_f = 0.0263 \text{ W/mK}$$

$$(\text{air @ 300 K}) \quad \nu = 15.89 \times 10^{-6} \text{ m}^2/\text{s}$$

$$Pr = 0.707$$

$$T_\infty = 293 \text{ K}$$

$$\text{Surroundings} : T_{\text{sur}} = 293 \text{ K}$$

The circuit board aspect ratio, defined as the total length of the board in the flow direction over the thickness of the board (L/t), is of the order 125:1. The predominant surfaces for convective cooling are the front and back surfaces of the circuit board, which encompass approximately 99% of the total exposed surface area of the circuit board. Therefore, the heat transfer through the edges of the circuit board is considered negligible and these surfaces will be treated as adiabatic.

Although the local convective heat transfer coefficient varies significantly over the surface of an electronic circuit board, local maximum values of h associated with natural convection cooling of typical PCBs range from approximately 5 to 20 W/m²K when air is used as the coolant fluid (Chu and Simons, 1984). As a result, typical values of the Biot Number ($Bi = ht/k_s$) in practical applications rarely become greater than 0.1. The

magnitude of the Biot number serves as an indication of the relative magnitude of the thermal resistance across the thickness of the circuit board to the thermal resistance within the fluid boundary layer. Since it is commonly accepted that a $Bi < 0.1$ allows a two-dimensional conduction analysis to be used with minimal deviation from results obtained using a more rigorous three-dimensional solution, a two-dimensional assumption will be used in the iterative model. For the present default case, this approximation is valid where the heat transfer coefficient h is less than $250 \text{ W/m}^2\text{K}$. This value is greater than the values observed even in many forced convection applications and as it will be seen, this is approximately 20 times greater than the local maximum values of h observed for the default case.

The cooling fluid is taken to be dry air with flow over the circuit board assumed to be steady, two dimensional and incompressible. The maximum flow velocity anticipated in microelectronic applications is low enough that the flow can be considered laminar and frictional dissipation can be considered negligible. The circuit board has a uniform thickness with heat dissipating component packages being in perfect contact with the surface of the circuit board. The power dissipated by the components is assumed to be steady and invariant with respect to time.

In the following section, the parametric behavior of the surface temperature variation and heat transfer characteristics of the circuit board will be discussed.

DISCUSSION

The three-dimensional plots in Fig. 3 show the distributions of the local Boussinesq number based on the convective heat flux, dimensionless temperature, and heat transfer coefficient for the default configuration where $k_s = 2 \text{ W/mK}$, $\epsilon = 0$, and $Q_{j1} = Q_{j2} = 1 \text{ W}$. The circuit board is cooled by natural convection with the gravity vector pointing in the negative x -direction leading to a buoyancy induced flow in the positive x -direction.

The temperature profile, as shown in Fig. 3b, is similar to what could be found in a low velocity forced convection application. But in natural convection the flow velocity increases in the positive x -direction as more heat is dissipated into the boundary layer. Unlike in forced flow applications where two heat sources of equal strength, arranged as in Fig. 2, always produces a higher peak temperature over the second source, in natural convection the downstream source can have a lower peak temperature than the upstream source because of the positional dependence of the flow velocity. This is due to the non-linear characteristic of the natural convection cooling and the lower peak temperature at the downstream source occurs when the circuit board conductivity is small and/or two heat sources are located far apart along the flow stream.

As shown in Fig. 3c, the heat transfer coefficient in conjugate natural convection applications is driven by the heat flux and as such the heat transfer coefficient in the immediate vicinity of the leading edge of the circuit board is approximately $4 \text{ W/m}^2\text{K}$, growing to a local maximum value of $12 \text{ W/m}^2\text{K}$ over the first source. This is in sharp contrast to forced convection, as shown by Culham et al. (1991a), where the value of the local heat transfer coefficient is observed to be decreasing monotonically from its maximum near the leading edge of the circuit board to its minimum of near zero in the downstream wake of the first source.

For the following discussions on the parametric behavior, the

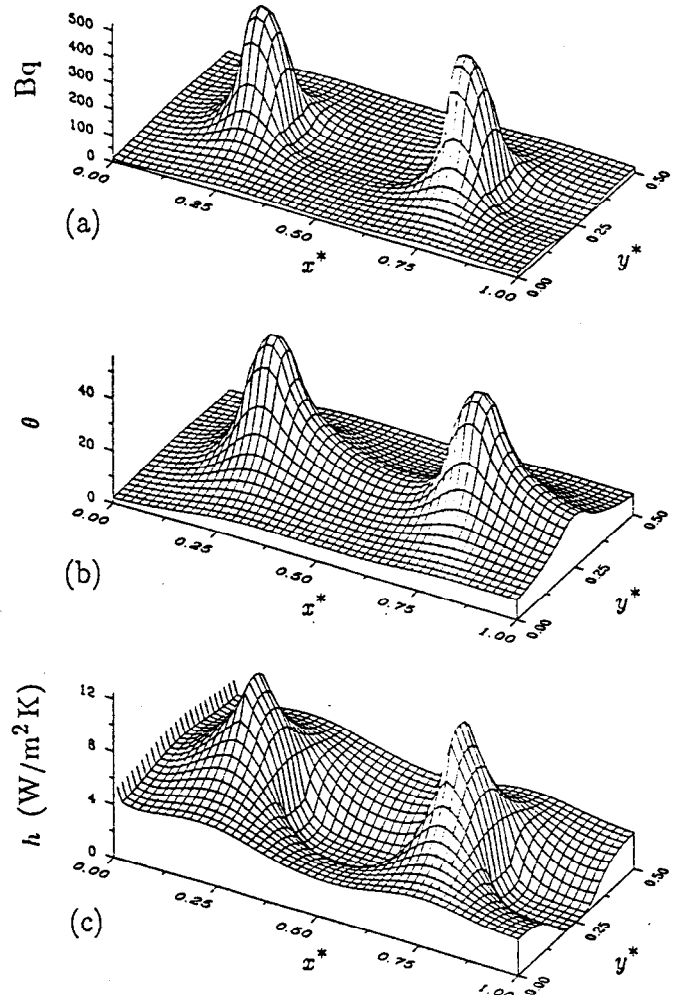


Fig. 3 Dimensionless surface heat flux and surface temperature distributions and local convective heat transfer coefficient for the default case ($k_s = 2 \text{ W/mK}$, $\epsilon = 0$, $Q_{j1} = Q_{j2} = 1 \text{ W}$).

above default case will be used as the reference configuration. As it was stated earlier there are five controllable dimensionless parameters on which the solutions depend. With physical dimensions of the circuit board and the values of thermophysical properties of air unchanged, the effects that the three remaining parameters, namely $k_s t/k_f L$, Bq_r , and Bq_j , have on the solutions will be examined by varying the board conductivity k_s , the surface emissivity ϵ , and the power dissipation and location of the leading heat source over a range typically observed in microelectronic applications. Figures 4-6 show the effect that thermal conductivity, emissivity and heat source strength have on the local value of the dimensionless surface temperature along the center line of the circuit board, where $\theta_c = \theta_w(y^* = 0.25)$.

Thermal Conductivity

The conduction of heat within a printed circuit board is described by Laplace's equation, as given in Eq. (7), which leads to the fin equation, as given in Eq. (15). when the appropriate interfacial conditions are applied. As seen in Eq. (15), the thermal conductivity of the solid, k_s , must be considered in the

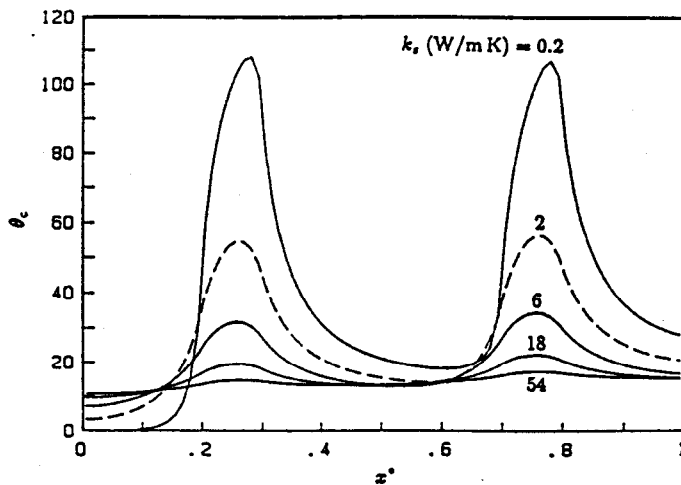


Fig. 4 Dimensionless surface temperature variation along the center line of the circuit board ($y^* = 0.25$) showing the effect of changes in board conductivity k_s , from 0.2 to 54 W/mK where $k_s = 2$ W/mK is the default case.

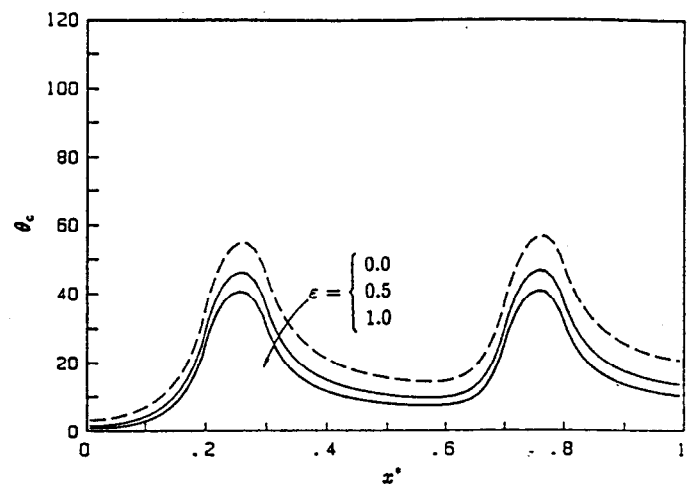


Fig. 5 Dimensionless surface temperature variation along the center line of the circuit board ($y^* = 0.25$) showing the effect of changes in board emissivity ϵ from 0 to 1 where $\epsilon = 0$ is the default case.

solution process, and it has a strong impact on the distribution of heat and therefore the distribution of temperature. Although most printed circuit boards are complex laminated structures, the present study assumes a constant value for the circuit board conductivity. A method can be employed to produce a single representative value of thermal conductivity for the full multilayered structure. The series and parallel heat flow paths must be considered, with the harmonic mean of the two resistive paths being used to calculate the effective thermal conductivity.

The thermal conductivity, as shown in Fig. 4, has a significant effect on the peak source temperature. Through the use of laboratory experiments and numerical simulation it can be seen that the conduction heat transfer in the solid must be considered even for low conductivity materials, such as plastics and fiberglass found in circuit board constructions. The default case, where $k_s = 2$ W/mK, is shown using the dotted line in Fig. 4.

When the thermal conductivity is low (i.e., $k_s < 0.2$ W/mK) the peak temperature of the downstream source is lower than that of the leading source. This phenomenon was first observed by Jaluria (1982) who solved the boundary layer equations by using finite difference methods for cases with a number of strip heat sources of uniform surface heat flux mounted flush on an adiabatic plate (i.e., $k_s = 0$ W/mK) in air. As the circuit board conductivity decreases, less heat is conducted away from the heat sources through the solid and more heat has to be dissipated directly into the fluid from the confined region at and near the sources. As it happens, the temperature of the leading heat source will increase significantly, resulting in an increase in the velocity of the buoyant driven flow in the boundary layer. The surface temperature decreases immediately after the first source but never becomes lower than the ambient fluid temperature. The positive fluid temperature excess represents an upward buoyant force on the fluid. A portion of this force will be used to overcome the friction, and the remainder will be used to accelerate the flow, resulting in a perpetual increase in the fluid velocity. If the two sources are far enough apart, the higher approaching velocity combined with decreasing wake temperature will lower the peak temperature of the downstream source below that of the leading source.

In the limit as the circuit board conductivity becomes zero, the boundary layer approximation in the energy equation and the assumption of negligible thermal diffusion in the planar directions become invalid also in the vicinity of the source edges. The problem is no longer a conjugate problem. As the circuit board conductivity increases on the other hand, the circuit board approaches an isothermal condition in the limit, representing the minimum temperature the heat sources can attain by means of changes in the thermal conductivity.

Surface Emissivity

Because the convective heat transfer coefficient in natural convection applications is generally less than 10 W/m²K, the component of heat dissipated by way of radiation is much more significant than in forced convection applications. It is not uncommon for up to 40% of the total heat generated to be dissipated by radiation.

A change in the surface emissivity of the circuit board has a similar effect on dimensionless temperature regardless of location, as shown in Fig. 5. The emissivity of the circuit board is assumed uniform for each case, with three cases examined: i) $\epsilon = 0$ (white body), ii) $\epsilon = 0.5$ (grey body) and iii) $\epsilon = 1.0$ (black body). The default case, where $\epsilon = 0$, is shown using the dotted line in Fig. 5.

Source Strength

Figure 6 shows the effect of a change in the heat flux of the upstream heat source on the dimensionless centerline temperature. An increase in heat flux at upstream locations is felt locally as evidenced by the increase in the peak temperature of the first heat source and to a smaller extent through the propagation of heat within the boundary layer at downstream locations. Unlike in the forced convection applications (Culham et al., 1991a), a close examination of the figure reveals that the rate of increase in the temperature of the first source with respect to Joulean heating diminishes as the level of heating increases. This corresponds to what was expected, since the temperature excess is known to be proportional to a 0.8 power of the convective heat

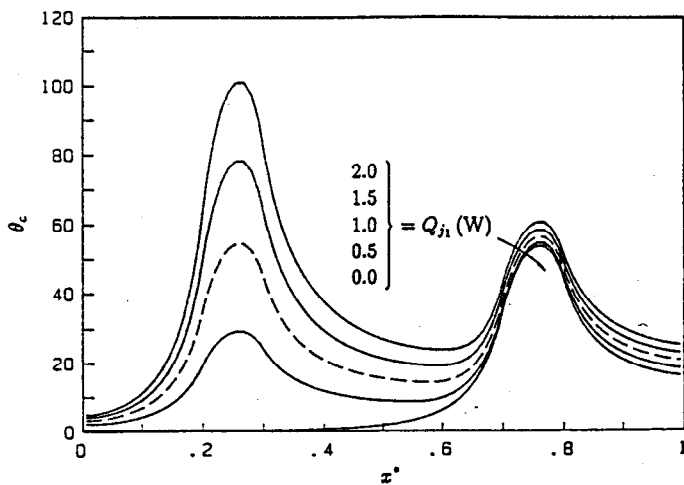


Fig. 6 Dimensionless surface temperature variation along the center line of the circuit board ($y^* = 0.25$) showing the effect of changes in power level of upstream source Q_{j1} from 0 to 2 W where $Q_{j1} = 1$ W is the default case.

flux, $(T - T_\infty) \propto q^{4/5}$, according to the boundary layer solutions. The default case, where $Q_{j1} = 1$ W, is shown using the dotted line in Fig. 6.

Source Location

Figure 7 shows how the dimensionless temperature of the second source is affected by a change in the location of the first source when it is moved between the leading and trailing edge of the circuit board, for different values of the circuit board conductivity. The abscissa is given as \bar{d} , which is defined as the distance between the centerline of the two heat sources divided by the source length ℓ . When $\bar{d} = 0$ the centerline of the two heat sources coincide and the two sources overlap giving the same effect as a single source of twice the source strength. The ordinate ϕ is defined as

$$\phi = \frac{\bar{T}_2 - \bar{T}_{2,0}}{\bar{T}_{2,0} - T_\infty} \quad (33)$$

where \bar{T}_2 denotes the average temperature of the second source, and $\bar{T}_{2,0}$ is \bar{T}_2 when the second source is the only source on the circuit board.

For a fixed thermal conductivity k_s , the maximum temperature occurs at $\bar{d} = 0$. When k_s becomes small and approaches 0 the circuit board becomes adiabatic, and the boundary layer theory indicates that the maximum value of ϕ should approach a value of 0.741. When k_s becomes large and approaches infinity the circuit board becomes isothermal, and the boundary layer theory indicates that the maximum ϕ is again 0.741. The figure reveals the proper behavior of the solutions as k_s approaches these limiting values.

Negative ϕ values are observed in the left end of the variation when $k_s = 0.2$ W/mK. This indicates that it is possible to obtain a lower temperature of the downstream source by adding a secondary source near the leading edge of the circuit board when the circuit board conductivity is small. This is due to the same non-linear phenomena that was discussed previously in Fig. 4.

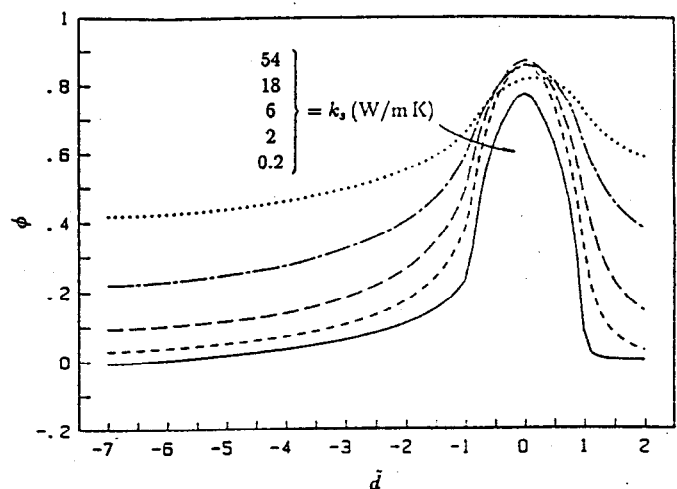


Fig. 7 Dimensionless average temperature of the downstream source as a function of the position of the other source for various k_s values, as the location of the other source varies from the leading edge to the trailing edge of the board.

Parameter Summary

Figure 8 is a summary of the effects of the thermal conductivity, surface emissivity of the circuit board and the source strength of the upstream source on the average Nusselt number of the downstream source which is defined by

$$Nu_2 = \frac{Q_{j2}}{(\bar{T}_2 - T_\infty)k_s \ell} \quad (34)$$

The multiple scales along the abscissa are arranged such that the node in the center of the curves corresponds to the default conditions. Therefore the heat transfer efficiency, as measured at the downstream heat source, can be compared for the full range of design conditions discussed herein.

A change in the thermal conductivity leads to the largest change in the Nusselt number, with a change of circuit board conductivity between the default setting of 2 W/mK and a value of 54 W/mK giving a three fold increase in the Nusselt number.

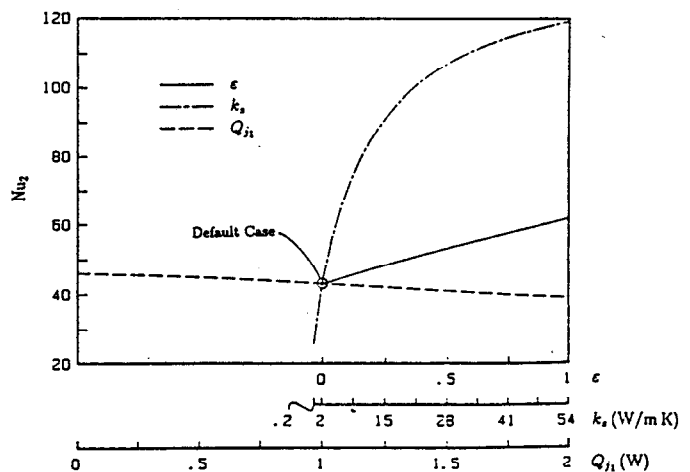


Fig. 8 Average Nusselt number variation of the downstream source as a function of k_s , ϵ , and Q_{j1} .

As the thermal conductivity becomes large the increase in the Nusselt number quickly diminishes due to the relative increase in the thermal resistance in the boundary layer. A change in the emissivity between 0 and 1 provides an increase in the Nusselt number of approximately 35%, while an increase in the heat flux of the first source reduces the Nusselt number of the second source by 10 - 15% due to the wake effect through the boundary layer.

Figure 9 summarizes the relative fraction of heat dissipation attributed to each of the three modes of heat transfer from both heat sources for the default circuit board (except the value of ϵ as indicated in the figure) with a thermal conductivity ranging from 0+ to 20 W/mK. When the thermal conductivity is greater than 1.0 W/mK conduction is the predominant mode of heat dissipation from the sources. For thermal conductivities of less than 0.2 W/mK, conduction still accounts for approximately 25% of the total heat transfer.

Figure 9 also shows the change in heat dissipation due to conduction, convection and radiation for changes in the surface emissivity of the circuit board. When the emissivity is increased the component of heat previously dissipated by conduction and convection is dissipated by radiation which may account for near 30% of the total heat dissipation from the heat sources. As can be seen from the figure when $\epsilon = 1.0$, the magnitude of radiation is comparable to that of convection throughout the range of k_s values presented.

CONCLUSIONS

The problem discussed in this paper is a specific example of a circuit board and heat source combination. The ability to analyze problems of a general nature can only be accomplished by conducting extensive laboratory experiments, which can be time consuming and extremely expensive to perform, or through the use of a general purpose conjugate model, such as META.

The thermal conductivity is found to be the most efficient parameter that can be controlled to lower the peak source tem-

peratures. The peak temperature and heat transfer performance of heat sources are most sensitive to the changes in the thermal conductivity when the circuit board conductivity is small. Therefore, the effect of conduction heat transfer through a circuit board can never be ignored and a conjugate model has to be solved to obtain correct predictions of heat transfer characteristics of a circuit board. The effect of radiation should be included also as radiation may account for a significant fraction of the total heat dissipation from heat sources as well as from entire circuit board surfaces.

ACKNOWLEDGMENTS

The authors wish to acknowledge the financial support of the Natural Sciences and Engineering Research Council of Canada under CRD contract 661-062/88.

REFERENCES

- Chu, R.C., and Simons, R.E., 1984, "Thermal Management of Large Scale Digital Computers," *Thermal Management Concept in Microelectronic Packaging; From Component to System*, ISHM Technical Monograph Series 6984-003, Section 4, Chapter 1, pp. 193-214.
- Culham, J.R., Lee, S., and Yovanovich, M.M., 1991a, "The Effect of Common Design Parameters on the Thermal Performance of Microelectronic Equipment: Part II - Forced Convection," ASME National Heat Transfer Conference, Minneapolis, MN, July 28-31.
- Culham, J.R., Lemczyk, T.F., Lee, S. and Yovanovich, M.M., 1991b, "META - A Conjugate Heat Transfer Model For Cooling of Circuit Boards With Arbitrarily Located Heat Sources," ASME National Heat Transfer Conference, Minneapolis, Minnesota, July 28-31.
- Jaluria, Y., 1982, "Buoyancy-Induces Flow Due to Isolated Thermal Sources on a Vertical Surface," *ASME Journal of Heat Transfer*, Vol. 104, pp. 223-227.
- Kishinami, K., and Seki, N., 1983, "Natural Convective Heat Transfer on an Unheated Vertical Plate Attached to an Upstream Isothermal Plate," *ASME Journal of Heat Transfer*, Vol. 105, pp. 759-766.
- Kishinami, K., Saito, H., and Tokura, I., 1987, "Natural Convective Heat Transfer on a Vertical Plate With Discontinuous Surface-Heating (Effect of Heat Conduction in Unheated Elements)," *Proceedings of ASME-JSME Thermal Engineering Conference*, Vol. 4, pp. 61-68.
- Lee, S., and Yovanovich, M.M., 1989, "Conjugate Heat Transfer From a Vertical Plate With Discrete Heat Sources Under Natural Convection," *ASME Journal of Electronic Packaging*, Vol. 111, pp. 261-267.
- Lee, S., and Yovanovich, M.M., 1991, "Linearization Method for Buoyancy Induced Flow Over a Non-Isothermal Vertical Plate," AIAA 26th Thermophysics Conference, Honolulu, Hawaii, June 24-26.
- Zinnes, A.E., 1970, "The Coupling of Conduction With Laminar Natural Convection From a Vertical Flat Plate With Arbitrary Surface Heating," *ASME Journal of Heat Transfer*, Vol. 92, pp. 528-535.

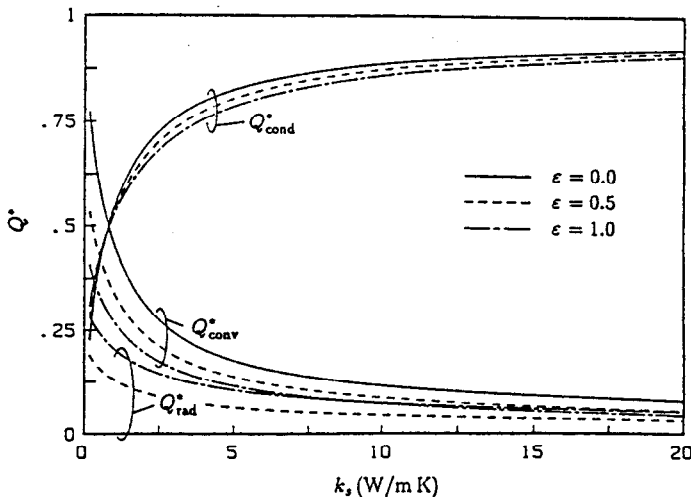


Fig. 9 Dimensionless heat dissipation from the downstream heat source by means of various modes of heat transfer, showing the relative magnitude of convection Q_{conv} , conduction Q_{cond} and radiation Q_{rad} as functions of k_s for different ϵ values.